



STRONGLY-INTERACTING ELECTROWEAK SECTOR AT FUTURE COLLIDERS ·

Tao Han

*Fermi National Accelerator Laboratory, P. O. Box 500
Batavia, IL 60510, USA*

ABSTRACT

If there are no light Higgs bosons found below $O(800 \text{ GeV})$ or so, the interactions among longitudinally-polarized vector bosons (W_L) will become strong at the TeV region, and new physics that is responsible for the electroweak symmetry breaking must emerge at this energy scale. We discuss the phenomenological prospects of the Strongly-interacting Electro-Weak Sector (SEWS) at future TeV linear colliders and hadronic supercolliders.

1. W -Boson Physics: from "Weak" to "Strong"

This year, 1993, is the twentieth anniversary of the experimental confirmation of the weak neutral current. It also marks the tenth anniversary of the observation of the W bosons (here and henceforth W generically denotes the W^\pm and Z bosons, unless specified otherwise). These discoveries demonstrated the major triumph of the $SU(2)_L \otimes U(1)_Y$ electroweak gauge structure. High energy experiments in the past two decades have further verified the validity of the Standard Model (SM) to high precision, including a constraint on the top-quark mass $m_t = 150_{-24}^{+19+15}_{-20} \text{ GeV}$.¹ We thus have been enjoying a beautiful theory that successfully describes all particle phenomena up to highest energy scale accessible today.

However, among several unanswered fundamental questions in the Standard Model, the elusive neutral scalar, the Higgs boson (H), predicted by the SM as the remnant of the spontaneous electroweak symmetry breaking, has not been observed. In fact, there is no direct experimental evidence so far in favor of any specific proposal for the mechanism of the electroweak symmetry breaking. This is clearly one of the most prominent mysteries of contemporary particle physics. Exploring the electroweak symmetry breaking sector is one of the most challenging tasks for high energy physicists, and it is one of the major motivations to build the next generation of colliders.

To study the electroweak symmetry breaking sector, it is instructive to first recollect the physics of weak bosons. One of the earlier examples of conventional weak interactions is the neutrino-nucleon scattering, $\bar{\nu}_e + p \rightarrow n + e^+$. It is described

¹Invited talk at the "2nd International Workshop on Physics and Experiments at Linear e^+e^- Colliders", Waikoloa, Hawaii, April 26-30, 1993.



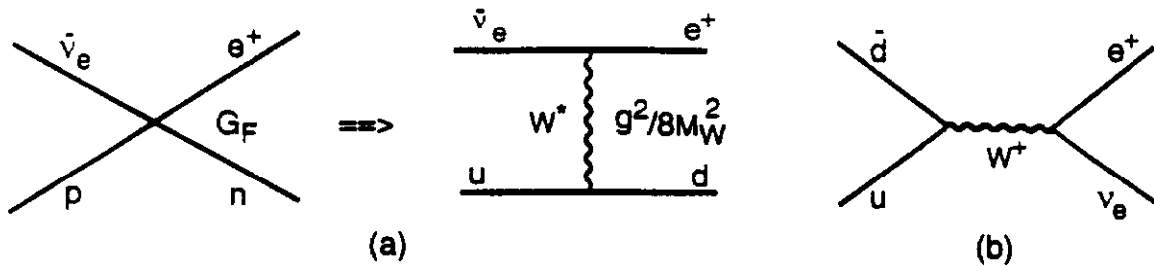


Figure 1: Representative Feynman diagrams for (a) low energy virtual W effect in $\bar{\nu}_e + p \rightarrow n + e^+$, and (b) nearly on-shell W^+ production at high energies.

well by the four-fermion contact interaction, and the amplitude goes like $G_F s$, where G_F is the Fermi weak-coupling constant and of order 10^{-5} GeV^{-2} , and s the squared c.m. energy. This amplitude would not respect unitarity at high energies. In the SM language, it is a neutrino-up-quark scattering via a highly off-shell W , as shown in Fig. 1(a). If $s \ll M_W^2$, the effective coupling reduces to the conventional one. $G_F/\sqrt{2} = g^2/8M_W^2$, where g is the $SU(2)_L$ coupling. We see that the smallness of the G_F value is nothing but the large- M_W suppression at the low energy. At collider energies, a nearly on-shell W^+ production and decay can be described by the same amplitude via $\bar{d}u$ annihilation (see Fig. 1(b)) as was already experimentally observed at the CERN $Spp\bar{S}$ and the Fermilab Tevatron. The effective coupling is characterized by g , and the W -propagator presents a proper high energy behavior. We have now learned two things: first, the conventional weak interactions are not intrinsically “weak”: they are weak because the energy available is much smaller than M_W ; second, the unitarity violation of four-fermion interactions at high energies is cured by introducing the intermediate vector bosons. The scale of M_W is the *first* threshold of the “weak” interactions.

If we keep going to an even higher energy scale at next generation of supercolliders, at which the squared c.m. energy $s \gg M_W^2$, the polarization vector of a longitudinally-polarized vector boson (W_L) can be approximated as $\epsilon_L^\mu \simeq p^\mu/M_W$, where p is its momentum, and the amplitude of pure $W_L W_L$ scattering goes like s/v^2 , where $v \simeq 246 \text{ GeV}$, is the vacuum expectation value of the scalar field. The interactions among the longitudinal weak bosons would therefore become strong and violate unitarity at about 1 – 2 TeV.^{2,3} Something must happen before or at this energy scale to cure the bad high energy behavior of $W_L W_L$ scattering and this will be the *second* threshold of the “weak” interactions.² It is the Higgs boson in the SM that comes in to rescue the situation: Higgs-boson exchange diagrams cancel the linear dependence on s , replaced by m_H^2 . This can be easily understood by invoking the electroweak “Equivalence Theorem”,²⁻⁴ which states that at high energies, the external longitudinal vector bosons in the scattering amplitudes recall their origin and can be replaced by the corresponding Goldstone bosons (w ’s). Since the self-coupling λ among the scalars (the Goldstone and the Higgs bosons) in the SM is proportional to m_H^2 , the scattering amplitude of $W_L W_L$, equivalent to that of the

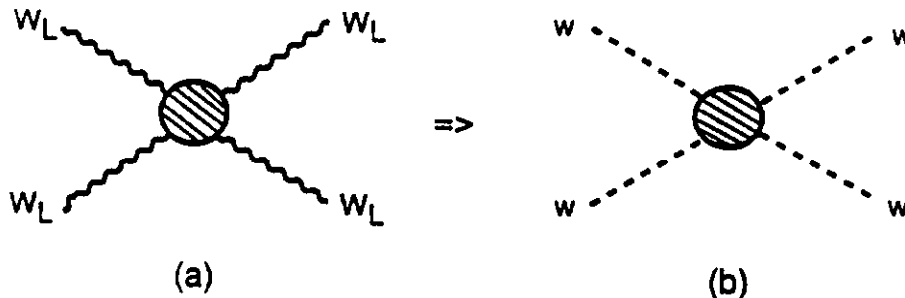


Figure 2: Symbolic diagrams for (a) longitudinally-polarized $W_L W_L$ scattering, and (b) equivalent Goldstone-boson ww scattering.

Goldstone bosons as symbolically shown in Fig. 2, goes like m_H^2/v^2 . In the SM, m_H is essentially a free parameter and the current experimental lower limit on m_H from LEP I data is about 60 GeV.⁵ Therefore, if there is no Higgs boson found below 800 GeV or so, the $W_L W_L$ scattering nevertheless becomes strong^{2,3,6,7} regardless what kind of new physics appears. This is the scenario of the Strongly-interacting Electro-Weak Sector (SEWS)^{8,9} that we will consider in this talk.

How do we expect to experimentally search for the SEWS? Obviously, any information about the SEWS must be from studies of the massive vector-bosons (W 's). Since we have been able to produce a large number of W 's, especially a million Z 's at LEP I, the precision measurements of electroweak parameters may provide important information about the higher-scale physics beyond the SM.¹⁰⁻¹² Indeed, from the "oblique" corrections for certain types of Technicolor models, significant limits can be found. However, these are not sensitive enough to other cases, such as those with scalar Higgs bosons.¹³ One can also consider to study the low energy effects from SEWS on vector-boson self-interactions, such as the triple-vector-boson vertices.¹⁴⁻¹⁶ However, as argued in Einhorn's talk,¹⁶ the expected deviation from the SM values of the vector-boson self-interactions may be only at a percentage level or less since the dependence on the cutoff where the new physics enters is at most logarithmic. Of course, the most direct way of studying the SEWS is to look at the $W_L W_L \rightarrow W_L W_L$ scattering at high energies, because these processes couple to the SEWS most strongly. In what follows, we will mainly discuss the phenomenology of $W_L W_L$ scattering at future colliders.

Before we proceed, two remarks are in order. First, an electroweak sector with light Higgs bosons is a weakly-coupled theory. The SM with a light Higgs boson is the simplest example of this type. The minimal supersymmetric model is another. These are clearly very attractive options and have been studied intensively both theoretically and phenomenologically, although there are still theoretical difficulties in these models. For recent reviews, see talks by Gunion and Kane in these proceedings.¹⁷ However, before a light Higgs boson is found, or any other strong experimental evidence is established, such as in searches of SUSY particles, we cannot simply ignore this seemingly more complex scenario of the SEWS, espe-

cially when guiding our experimental designs. After all, low-energy hadron physics is messy and QCD in that energy regime is not as simple as one could have hoped. But Nature has been mean to us at least once!

Secondly, it has been argued that the SM is not a consistent effective theory if $m_H \gtrsim 800$ GeV or so,¹⁸ based on the triviality argument and lattice simulations. We may nevertheless discuss the SM and its generalization with a TeV Higgs boson as a prototype for models with SEWS.

In the following, we first review in Section 2 some representative models and schemes in which the SEWS occurs. We then discuss the feasibility of experimentally studying the SEWS at future linear colliders and hadronic supercolliders in Sections 3 and 4, respectively. We summarize in Section 5.

2. Models and Schemes in Studying SEWS

There is little experimental guidance thus far on the underlying dynamics responsible for the generation of mass. However, there is a piece of information that provides important understanding to the EW sector. Experimentally, the ρ -parameter¹⁹ is very close to unity, which implies that $M_W \simeq M_Z \cos\theta_W$ to rather high precision. This relation holds automatically if there are only Higgs doublets in the model. In more general models, it is naturally protected if there is a global $SU(2)$ symmetry. In this talk, we will assume the so-called “custodial” symmetry²⁰ of $SU(2)_V$ broken from global $SU(2)_L \otimes SU(2)_R$, and that the corresponding Goldstone bosons, w^\pm and z , form an “isospin”-triplet, formally analogous to π^\pm and π^0 in the low-energy strong interactions.

In this section, we first discuss some implications of SEWS. We then discuss several representative models and schemes which we will adopt in the later phenomenological analyses. We will restrict our attention to models with spin $J = 0$ and isospin $I = 0$ resonances (the Higgs-boson-like, called scalar-dominance), and $(J, I = 1, 1)$ resonances (the techni-rho-like, called vector-dominance), as well as non-resonant models in $W_L W_L$ scatterings.

2.1. Implications of SEWS

We believe that the Goldstone bosons transform under the $SU(2)_V$ as a triplet. But we do not have any satisfactory theories that are consistent with experimental constraints to describe the dynamics of a Strongly-interacting Electro-Weak Sector, or the possibly strong interactions among the Goldstone bosons. Furthermore, technically, the perturbation theory may have broken down in the SEWS, so that there is no reliable way of performing theoretical calculations. Unitarization of $W_L W_L$ scattering amplitudes based on certain models may be necessary, which makes the predictions unitarization-scheme dependent. Experimentally, the conventional bump-hunting method may not work in studying $W_L W_L$ scattering due to very broad resonances or even structureless (nonresonance) in the invariant mass spectrum, which are common in SEWS.

While we know very little about the SEWS indeed, we do have some general information about scattering matrix elements of the Goldstone bosons in the SEWS. First, based on group theory arguments of $SU(2)_V$, all scattering matrix elements are determined by only one amplitude function $A(s, t, u)$, where s, t , and u are the kinematical variables. They are given by

$$\begin{aligned}
\mathcal{M}(W_L^+ W_L^- \rightarrow Z_L Z_L) &= \mathcal{M}(Z_L Z_L \rightarrow W_L^+ W_L^-) = A(s, t, u) \\
\mathcal{M}(W_L^+ W_L^- \rightarrow W_L^+ W_L^-) &= A(s, t, u) + A(t, s, u) \\
\mathcal{M}(Z_L Z_L \rightarrow Z_L Z_L) &= A(s, t, u) + A(t, s, u) + A(u, t, s) \\
\mathcal{M}(W_L^\pm Z_L \rightarrow W_L^\pm Z_L) &= A(t, s, u) \\
\mathcal{M}(W_L^\pm W_L^\pm \rightarrow W_L^\pm W_L^\pm) &= A(t, s, u) + A(u, t, s),
\end{aligned} \tag{1}$$

which satisfy the crossing relations. Secondly, at low energies when the c.m. energy is much smaller than the minimum of the lowest resonance and the electroweak scale $4\pi v$, the scattering amplitudes obey the low-energy theorems (LET),²¹ which are solely determined by the global symmetries before and after the spontaneous symmetry breaking. With our assumption of $SU(2)_V$, the LET amplitude is

$$A(s, t, u) = s/v^2. \tag{2}$$

Finally, the amplitudes must respect partial wave unitarity at all energies. That is about all we can safely say and we are ignorant of the detailed physics.

An important fact is that the background processes to the SEWS effects in the SM are in principle perturbatively calculable. So the search strategy is to understand the SM expectations as well as we can; to search for deviations from the SM prediction; and then to extract the underlying dynamics.

2.2. The $O(2N)$ Model

This first model represents an attempt to describe a Higgs boson in the nonperturbative domain at $\mathcal{O}(1 \text{ TeV})$. In the SM, the scalar self-coupling $\lambda \sim m_H^2$. A heavy Higgs particle corresponds to a large value of λ . For $m_H \gtrsim 1 \text{ TeV}$, naive perturbation theory breaks down, and one must take a more sophisticated approach.

One possibility for exploring the nonperturbative regime is to exploit the isomorphism between $SU(2)_L \otimes SU(2)_R$ and $O(4)$.²² Using a large- N approximation, one can solve the $O(2N)$ model for an arbitrary value of λ , to leading order in $1/N$. The theory can be characterized by a scale Λ of the Landau pole, below which it is a self-consistent effective theory. Large values of Λ correspond to small couplings λ and relatively light Higgs particles. In contrast, small values of Λ correspond to large λ and describe the nonperturbative regime.

It is not hard to show that the $W_L W_L$ scattering amplitudes respect the unitarity condition for all energies below Λ . In the following phenomenological discussions, we will take $N = 2$ and $\Lambda = 3 \text{ TeV}$. If we parameterize the position of the pole by its ‘‘mass’’ M and ‘‘width’’ Γ through the relation $s = (M - i\Gamma/2)^2$, then

$M \sim 0.8 \text{ TeV}$ and $\Gamma \sim 600 \text{ GeV}$.⁹

2.3. The Chirally-Coupled Scalar Model

The second model describes the low-energy regime of a technicolor-like model whose lowest resonance is a techni-sigma, at about $\mathcal{O}(1 \text{ TeV})$. The effective Lagrangian for such a resonance can be constructed using the techniques of Callan, Coleman, Wess, and Zumino.²³ The resulting Lagrangian is consistent with the chiral symmetry $SU(2)_L \otimes SU(2)_R$, spontaneously broken to the diagonal $SU(2)_V$. We will skip the details⁹ of constructing the chiral Lagrangian, which contains interactions among a new scalar field S and the Goldstone fields.

There are two free parameters in the Lagrangian, which can be traded for the mass (M_S) and the width (Γ_S) of the S . If we assume that S dominantly decays to a pair of Goldstone bosons, the width is then given by

$$\Gamma_S = \frac{3g_S^2 M_S^3}{32\pi v^2}. \quad (3)$$

For $g_S = 1$, the S reduces to the Higgs boson H in the SM. For $g_S \neq 1$, however, the S is *not* a typical H . It is simply an isoscalar resonance of arbitrary mass and width. In either case, one must check that the scattering amplitudes are unitary up to the energy of interest.

In what follows, we will choose $M_S = 1.0 \text{ TeV}$, $\Gamma_S = 350 \text{ GeV}$. These values give unitary scattering amplitudes up to 2 TeV .⁹

2.4. The Chirally-Coupled Vector Model

This example provides a relatively model-independent description of the techni-rho resonance that arises in most technicolor theories. As above, one can use the techniques of nonlinear realizations to construct the most general coupling consistent with chiral symmetry.²³ We will not present the detail discussions⁹ here to construct the chiral Lagrangian involving interactions among the new vector field (the techni-rho) and Goldstone fields.

There are two free parameters in the Lagrangian, g_V and a . They once again can be traded for the mass (M_V) and the width (Γ_V) of the new vector field.

$$M_V^2 = ag_V^2 v^2, \quad \Gamma_V = \frac{aM_V^3}{192\pi v^2}. \quad (4)$$

Because of the chiral symmetry, these two parameters completely define the theory. In the limit $g_V \rightarrow \infty$ and M_V finite, it implies $a \rightarrow 0$. The techni-rho V_μ decouples from ordinary fields, so that the SM is recovered.

The approach described above is essentially the same as the so-called BESS model.²⁴ There are two minor differences here. We have ignored a possible direct coupling term between the techni-rho and the fermions, which is called the parameter b . Also, we parameterize the theory by the mass M_V and the width Γ_V , while they choose the mass and the new coupling constant $g'' (= 2g_V)$. It is easy to work

out the relationships between these two different choices:

$$\Gamma_V = \frac{M_V^5}{192\pi g_V^2 v^4}, \quad g^2/g_V^2 = 768\pi v^2 M_W^2 \Gamma_V / M_V^5. \quad (5)$$

In what follows we will choose $M_V = 1$ (2) TeV, $\Gamma_V = 25$ (700) GeV, called Vector 1.0 (2.0), for studies at e^+e^- (pp) colliders. These values preserve unitarity up to 3 TeV and are consistent with experimental constraints.^{25,26}

2.5. Chiral Lagrangian Approach - Nonresonant

As seen in the discussions of the previous two examples, effective field theories provide a useful formalism to describe resonances in $W_L W_L$ scattering beyond the Standard Model in a relatively model-independent way. They also can be used to describe nonresonant models in which the $W_L W_L$ scattering occurs below the threshold for resonant production. The effective Lagrangian description allows one to construct scattering amplitudes that are consistent with crossing and chiral symmetry.^{27,15}

The most important effects at high energies can be found by considering the Lagrangian for the Goldstone fields,

$$\begin{aligned} \mathcal{L}_{\text{Goldstone}} &= \frac{v^2}{4} \text{Tr} \partial_\mu \Sigma^\dagger \partial^\mu \Sigma \\ &+ L_1 \left(\frac{v}{\Lambda} \right)^2 \text{Tr}(\partial_\mu \Sigma^\dagger \partial^\mu \Sigma) \text{Tr}(\partial_\nu \Sigma^\dagger \partial^\nu \Sigma) \\ &+ L_2 \left(\frac{v}{\Lambda} \right)^2 \text{Tr}(\partial_\mu \Sigma^\dagger \partial_\nu \Sigma) \text{Tr}(\partial^\mu \Sigma^\dagger \partial^\nu \Sigma), \end{aligned} \quad (6)$$

where $\Lambda \lesssim 4\pi v$ denotes the scale of the new physics.

The Lagrangian above describes new physics at energies below the mass of lightest new particles. To order p^2 in the energy expansion, only one operator contributes, and its coefficient is universal which is determined by the low-energy theorems (LET). All the effects of the new physics are contained in the coefficients of the higher-dimensional operators built from the Goldstone fields. To order p^4 , there are two additional operators that contribute to $W_L W_L$ scattering. In a sense, this approach is a model-independent parameterization of the new physics.

The difficulty with this approach is that the scattering amplitudes violate unitarity between 1 and 2 TeV. This indicates that new physics is near, but there is no guarantee that new resonances lie within reaches of the next generation colliders. The amplitudes have to be unitarized. For simplicity, we follow Chanowitz and Gaillard,³ take the LET amplitudes, and unitarize them by saturating the unitarity limit when they reach the bound $|a_i^J| < 1$ (called LET CG). This simple treatment is numerically not much different from the K -matrix method.⁹

2.6. N/D Approach

Recently, Hikasa and Igi proposed a model-independent scheme²⁸ to study SEWS. They construct amplitudes for the $W_L W_L$ scattering with scalar or vector

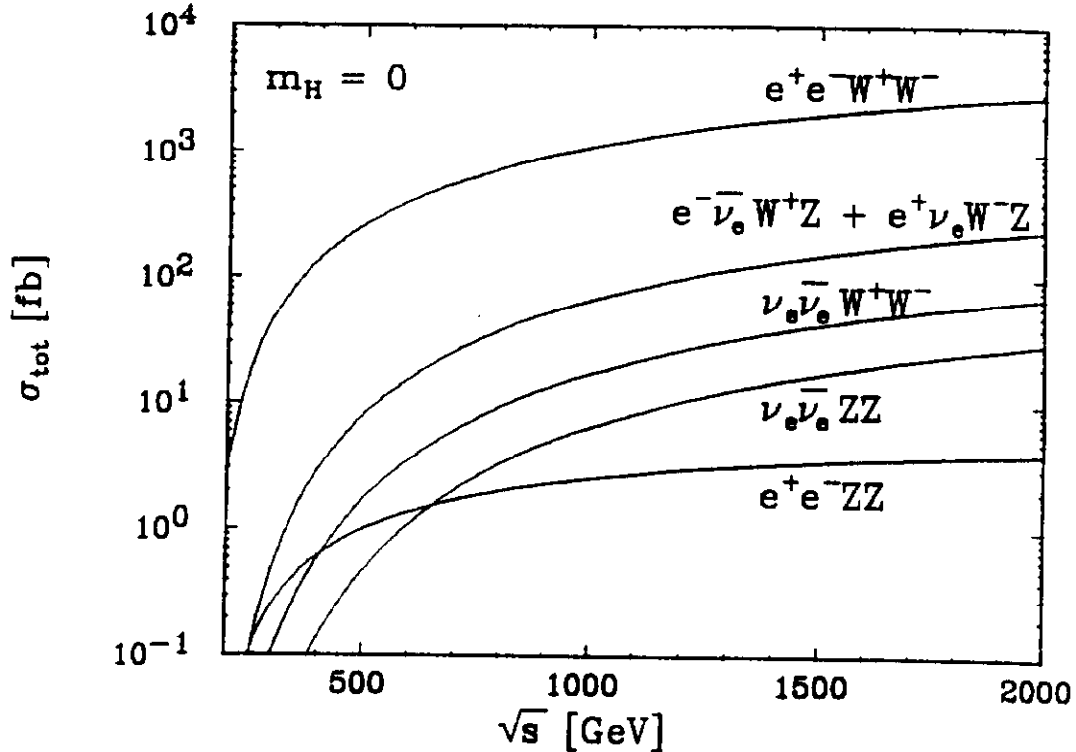


Figure 3: Total cross sections for the $e^+e^- \rightarrow f\bar{f}'WW'$ processes in the SM with $m_H = 0$.

resonances in a framework of self-consistent N/D method. The amplitudes satisfy unitarity, analyticity, and approximate crossing symmetry. This scheme could provide a convenient basis for phenomenological studies of SEWS below a typical scale about $4\pi v \simeq 3$ TeV.

3. SEWS at TeV Linear Colliders

We now discuss the feasibility of studying the SEWS at future TeV linear colliders.

3.1. Via $W_L W_L$ Fusion Processes

The $W_L^+ W_L^-$ fusion process dominates the heavy Higgs boson production at TeV e^+e^- colliders.^{29,30} More recently, two groups re-examined the heavy Higgs boson signal and backgrounds with a full set of SM diagrams.^{31,32} Figure 3 shows the expected total cross sections versus \sqrt{s} for the $e^+e^- \rightarrow f\bar{f}'WW'$ processes³² in the SM. The results were obtained with $m_H = 0$, so that they can be viewed as the irreducible SM backgrounds to the SEWS.

The final state W_L -pairs from the SEWS are central, and populated in the large M_{WW} region. The transverse momentum of the pair, $p_T(WW)$, is of order M_W

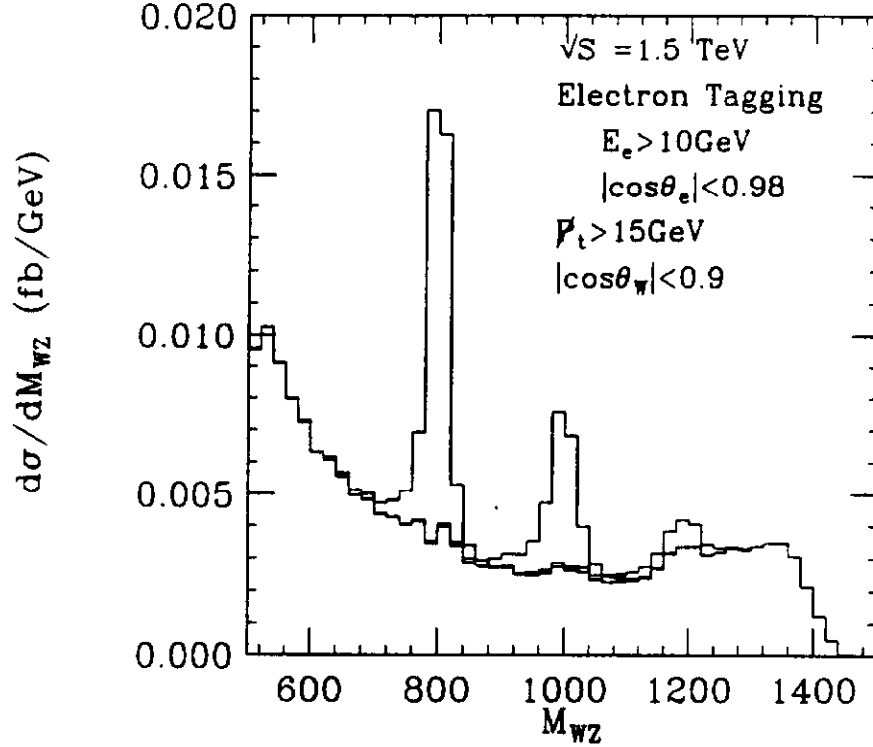


Figure 4: Invariant mass distribution of WZ in the $e^+e^- \rightarrow e^\pm\nu_e W^\mp Z$ process for signals of $M_V = 0.8, 1, \text{ and } 1.2$ TeV, and the continuum SM background.

(see Section 4 for more discussion). To observe a heavy Higgs-boson signal from the fusion processes, the basic kinematical cuts are

$$M_{WW} > 500 \text{ GeV}, p_T(WW) > 50 \text{ GeV}, |\cos(\theta_W)| < 0.6. \quad (7)$$

Processes of WW' plus an e^\pm in the final state are dominantly induced by nearly on-shell photons, and the rates for these processes are larger. To suppress these backgrounds, besides the cuts in Eq. 7, electron-vetoing has been found effective³² and the requirement is that

- no energetic e^\pm with $E_e > 50$ GeV in central region $|\cos(\theta_e)| < |\cos(0.15 \text{ rad})|$.

With these cuts, they found that at $\sqrt{s} = 1.5$ TeV the signals for $m_H = 1$ TeV in the processes $e^+e^- \rightarrow \nu_e\bar{\nu}_e W^+W^-$ and $e^+e^- \rightarrow \nu_e\bar{\nu}_e ZZ$ are clearly above the SM continuum backgrounds. For the case of $m_H \rightarrow \infty$ (LET), the signal is structureless in the M_{WW} spectrum and the background rate is comparable. Higher c.m. energy or a few hundred fb^{-1} of integrated luminosity is needed to see the statistical significance of the signal.³¹⁻³³

Kurihara reported their recent studies³⁴ on a scalar and a vector resonance based on the self-consistent N/D approach.²⁸ After some kinematical cuts³⁴ to separate the backgrounds, he concluded that with $\sqrt{s} = 1.5$ TeV and $\mathcal{L} = 200 \text{ fb}^{-1}$, a 1 TeV scalar (via W^+W^- final state) or a vector (via $W^\pm Z$ channel) can be observed

Table 1: Number of $W_L W_L$ events calculated for linear colliders at 1.5 (2.0) TeV, assuming an integrated luminosity of 200 (300) fb^{-1} .

	$O(2N)$	Scalar 1.0	Vec 1.0	LET	Bckgrnds
$e^+e^- \rightarrow \nu_e \bar{\nu}_e W_L^+ W_L^-$	320 (1050)	166 (570)	72 (270)	48 (165)	90 (255)
$e^+e^- \rightarrow \nu_e \bar{\nu}_e Z_L Z_L$	220 (690)	150 (480)	70 (204)	88 (330)	74 (216)
$e^-e^- \rightarrow \nu_e \nu_e W_L^- W_L^-$	50 (153)	70 (225)	70 (204)	88 (330)	202 (525)

as a resonance, with a few tens of events. Figure 4 shows the invariant mass distribution for a vector resonance in $W^\pm Z$ channel at $\sqrt{s} = 1.5$ TeV. For $M_V > 1$ TeV, the background in this channel becomes large and higher energies and luminosities would be needed to see the SEWS effects. However, more selective kinematical cuts may be helpful to improve the situation.

To have a more coherent picture, in Table 1 we present the expected number of events for $W_L^+ W_L^-$ and $Z_L Z_L$ final states via $W_L^+ W_L^-$ fusion for models discussed in Sec. 2. The results are for $\sqrt{s} = 1.5$ (2.0) TeV, assuming that the corresponding annual integrated luminosity is 200 (300) fb^{-1} , which is from a rescaling of a 500 GeV NLC with 20 fb^{-1} to keep a roughly constant event rate for $\sigma_{point} = 4\pi\alpha^2/3s \simeq 100 \text{ fb}/(E_{cm} \text{ TeV})^2$. The kinematical cuts used here are listed in Eq. 7. Since we have used the ‘‘Effective W -boson Approximation’’³⁵ for the signal calculation, the $p_T(WW)$ cut cannot be implemented directly. Instead, we take a 75% efficiency for this cut based on exact matrix element simulations. The $Z_L Z_L$ fusion diagrams have been ignored due to the much smaller neutral current coupling of e^\pm . The background estimates are obtained from the results of $m_H = 0$ by Hagiwara *et al.*,³² Although the signal rates are not very large and the backgrounds are comparable, it seems possible to observe statistically significant signal for any of the models at $\sqrt{s} = 1.5$ TeV with a few hundred fb^{-1} integrated luminosity.

Another interesting option is an e^-e^- collider.³⁶ The event rates for $e^-e^- \rightarrow \nu_e \nu_e W_L^- W_L^-$ for different models are also listed in Table 1, with the same kinematical cuts. This is a ‘‘pessimistic’’ channel in the sense that there is no resonant contribution to this channel in any model discussed. For instance, in a scalar-dominance model, $\sigma(W_L^- W_L^-)$ is significantly smaller than those of $W_L^+ W_L^-$ and $Z_L Z_L$ final states. Note that for nonresonant channels, $\sigma(W_L^- W_L^- \rightarrow W_L^- W_L^-) = \sigma(W_L^+ W_L^- \rightarrow Z_L Z_L)$ due to the crossing symmetry of Eq. 1. The irreducible background (with $m_H = 0$) is estimated³⁷ to be moderately larger than the signal, as given in Table 1. If we assume that other backgrounds such as $e^-e^- \rightarrow e^-e^- W^+ W^-$ (relevant for hadronic decay modes) via nearly real photons can be effectively suppressed by the $p_T(WW)$ cut plus an electron-veto,³² we see from the table that we may also be able to observe statistically significant signal at $\sqrt{s} = 1.5$ TeV with a few hundred fb^{-1} integrated luminosity.

We should point out that there is another potential background, $e^+e^- \rightarrow e^\pm \nu W^\mp Z$, which is not included in Table 1. The rate of this background is comparable to the signal with the cuts of Eq. 7 and the electron-veto,³² and we hope to separate

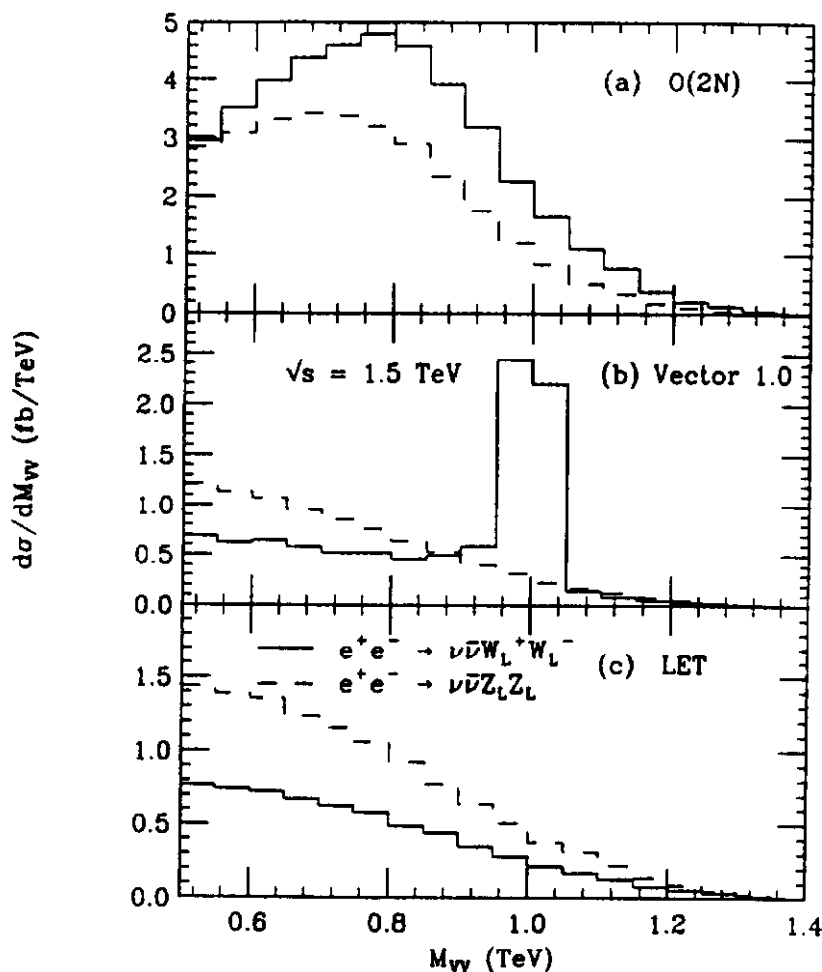


Figure 5: Invariant mass distributions of M_{VV} at 1.5 TeV for the processes $e^+e^- \rightarrow \nu_e \bar{\nu}_e W_L^+ W_L^-$ (solid), and $\nu_e \bar{\nu}_e Z_L Z_L$ (dashed), (a) $O(2N)$ model: (b) chirally-coupled vector model: (c) LET amplitudes.

it by distinguishing the W^\pm 's from Z 's in the final state. How well can we tell a W^\pm from a Z experimentally at the TeV e^+e^- colliders? Of course, the charged leptonic decay modes of e and μ can be easily used, but the branching fractions are rather small. It has been suggested³⁸ to tag a b -quark from $Z \rightarrow b\bar{b}$, with a branching fraction of 15%; while there is essentially no b from W^\pm -decay since the top-quark is heavier than the W^\pm . However, the largest branching fraction is the decay to light quarks (about 70%). It would be very advantageous if one can make use of the hadronic decay modes. Assume that the energy resolution of the hadronic calorimeter is³⁹

$$\Delta E_{hadron} = 35\% \sqrt{E} \oplus 2\% E,$$

then, naively, the uncertainty of the hadronic energy from the decay of a 500 GeV W is about 12 GeV. This is as large as the intrinsic W^\pm - Z mass difference, so that it is difficult to differentiate W^\pm 's from Z 's by measuring the di-jet mass of the decay

products. However, if we can combine the tracking information of the hadrons at the same time, great improvement in the di-jet mass construction should be possible.

If the SEWS effects are observed, it is then desirable to identify different models to uncover the underlying dynamics. We find once again that effectively distinguishing the W^\pm 's from Z 's is essential to serve this purpose. This is demonstrated in Fig. 5, where we plot the invariant mass distributions for the processes $e^+e^- \rightarrow \nu_e\bar{\nu}_e W_L^+ W_L^-$ and $\nu_e\bar{\nu}_e Z_L Z_L$ at 1.5 TeV for three models: (a) the $O(2N)$ model; (b) the chirally-coupled vector model (Vector 1.0); and (c) the LET amplitude. For a scalar-dominance model, we expect that the $W_L^+ W_L^-$ rate is larger than the $Z_L Z_L$ mode, like the case of the SM Higgs boson, although the resonance structure may not be clear. There will be a significant resonant enhancement for a vector-dominance model in the $W_L^+ W_L^-$ mode, but not in that of $Z_L Z_L$, just like $\rho^0 \rightarrow \pi^+ \pi^-$ only. However, if the resonances are far from our reach, then the LET amplitudes go like $-u/v^2$ for $w^+ w^-$ and s/v^2 for zz , so that $\sigma(w^+ w^- \rightarrow zz)/\sigma(w^+ w^- \rightarrow w^+ w^-) = 3/2$. The $Z_L Z_L$ rate is then larger than that of $W_L^+ W_L^-$, and more so in the central region. Measuring the relative yields of $W_L^+ W_L^-$ and $Z_L Z_L$ will reveal some hints for the SEWS. Although it may be a challenge to separate hadronic W^\pm and Z events, it is clearly important in studying the SEWS.

It has been argued⁴⁰ that if there are many particles other than the three Goldstone bosons (w^\pm, z) in the SEWS, the *elastic* scattering amplitudes for $W_L W_L \rightarrow W_L W_L$ may be significantly reduced. And the *inelastic* scatterings, although strong, may be lack of discernible resonant structure. The large inelastic channels themselves may be difficult to detect at the hadronic supercollider environment. This is the scenario of the ‘‘Hidden symmetry-breaking sector’’. However, in the rather clean environment at e^+e^- colliders, it is possible to study the inelastic channels directly. Although very much model-dependent, the final states in the inelastic channels are most likely pseudo-Goldstone bosons (ϕ 's), which would dominantly decay to heavy fermion pairs that are kinematically accessible.

$$W_L^+ W_L^- \rightarrow \phi_i \phi_j \rightarrow f_i \bar{f}_i, f_j \bar{f}_j.$$

The experimental signature then will be

- large missing transverse momentum, $p_T \simeq M_W$, resulting from $W_L^+ W_L^-$ fusion;
- four high- p_T jets with two pairs reconstructing the masses of the parent pseudo-Goldstone bosons: $M_{f_i \bar{f}_i} \simeq M_{\phi_i}$, $M_{f_j \bar{f}_j} \simeq M_{\phi_j}$.

Therefore, if a good hadronic mass resolution can be achieved, in contrast to the hadronic supercolliders, those events from inelastic channels in the ‘‘Hidden symmetry-breaking sector’’ could be spectacular.

3.2. Via e^+e^- Annihilation Processes

$W_L W_L$ fusion processes can go through different resonant channels, so that they provide direct studies on the underlying physics. However, the major disadvantage of this type of processes is the inefficiency of using the machine energy due

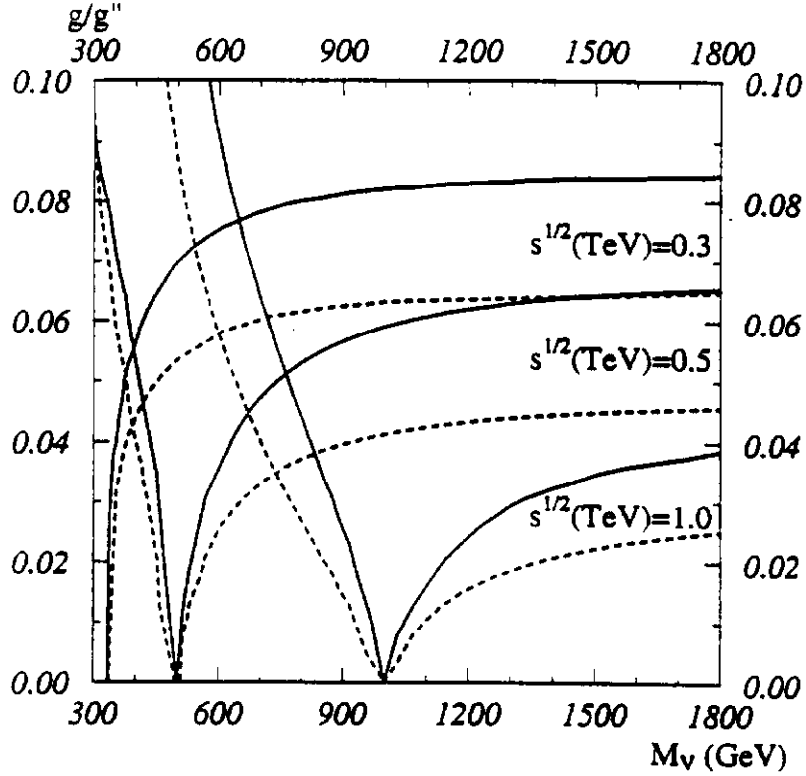


Figure 6: 90% C. L. contours in the plane $(M_V, g/g'')$ for c.m. energies at 0.3, 0.5, 1 TeV, $\mathcal{L} = 20 \text{ fb}^{-1}$ and $b = 0$. The solid lines correspond to the bound from the unpolarized WW differential cross section, the dashed lines to the bound from all the polarized differential cross sections $W_L W_L$, $W_T W_L$, $W_T W_T$ combined with the WW left-right asymmetries. The lines give the upper bounds on g/g'' .

to the loss of energy carried out by the spectator leptons after radiating W_L 's. It is conceivable to make the full use of the collider energy for vector resonant channels.

If $\sqrt{s} \simeq M_V$, then the vector resonance V can be produced by e^+e^- annihilation via either the direct $e\bar{e}V$ coupling or via $W - V$ mixing. Dominici presented their updated study²⁶ on the limits of BESS model parameters at the NLC of $\sqrt{s} \sim 0.3\text{--}2$ TeV. The processes of $e^+e^- \rightarrow W^+W^-$ and $e^+e^- \rightarrow f\bar{f}'$ have been studied and variables such as the total cross sections, forward-backward and left-right asymmetries are used to constrain the virtual V effects. Figure 6 shows the 90% C. L. upper limits on the $(M_V, g/g'')$ parameter plane at different assumed collider energies, where $g'' = 2g_V$ in Eq. 4. One sees that the NLC will be fairly sensitive to the BESS model parameters.

Another possible way of exploring the SEWS is via the final state interactions (FSI) of the W_L -pairs produced in e^+e^- annihilation. The FSI can be described by

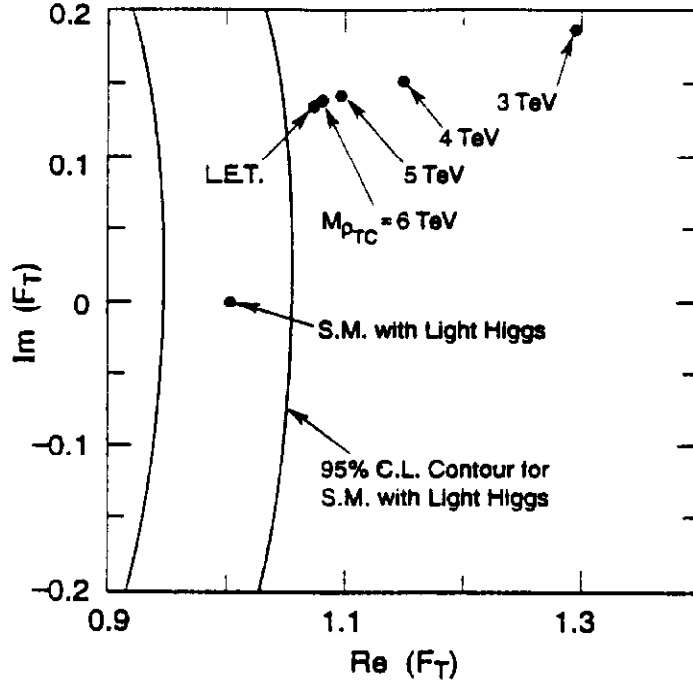


Figure 7: 95% C. L. contour for $Re(F_T)$ and $Im(F_T)$ at c.m. energy 1.5 TeV and $\mathcal{L} = 500 \text{ fb}^{-1}$.

an Omnés function^{41,38} and the rescattering coefficient F_T is given by

$$F_T = \exp\left[\frac{1}{\pi} \int_0^{\infty} ds' \delta(s') \left\{ \frac{1}{s' - s' - i\epsilon} - \frac{1}{s'} \right\}\right] \quad (8)$$

where $\delta(s)$ is the phase shift and characterizes the dynamics.^{38,41,42} Barklow updated his study on FSI via a techni-rho-like vector resonance in the $e^+e^- \rightarrow W^+W^-$ process.⁴² Figure 7 shows the SM expectation, a 95% C. L. contour, and a techni-rho contribution of different masses at $\sqrt{s} = 1.5 \text{ TeV}$ and an integrated luminosity of 500 fb^{-1} . One should be able to clearly see the contribution from a techni-rho with $M_V > \sqrt{s}$, and even possibly to distinguish the weakly-interacting SM from SEWS with a few years of data.

Basdevant *et al.*⁴³ recently argued that the above analysis corresponds to a Vector-Meson-Dominance coupling of a techni-rho resonance. Generically, the FSI will result in destructive interference between diagrams with and without rescattering, so that the differential cross section could develop a dip near the resonance region, instead of a bump. This may make the experimental observation more difficult and it deserves further study.

We have seen that the e^+e^- annihilation processes (*e. g.* the BESS model and the FSI) are more advantageous in searching for the SEWS effects, because of the full use of the collider energy, and correspondingly less backgrounds. However, it is essentially limited to a vector-dominance model of the $(I, J = 1, 1)$ channel. In other

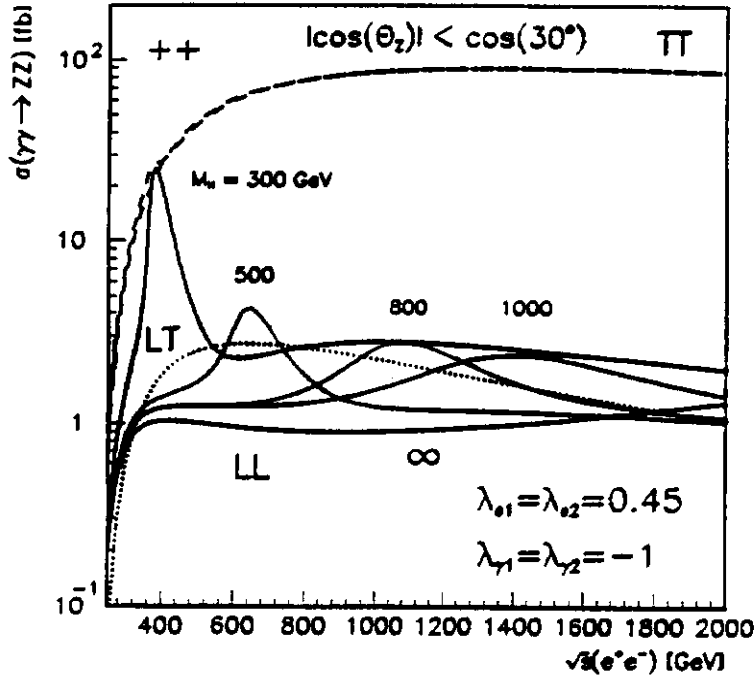


Figure 8: Total cross section of $\gamma\gamma \rightarrow ZZ$ versus $\gamma\gamma$ c.m. energy in units of fb for several heavy Higgs boson masses.

words, we would not expect to see significant effects in the annihilation channel if there is no neutral vector resonance to contribute.

3.3. TeV $\gamma\gamma$ Colliders

Due to the recently developed idea of back-scattered laser beam technique,⁴⁴ it is possible to build a $\gamma\gamma$ collider with similar energy and luminosity to the e^+e^- one. With appropriate choice of the $\gamma\gamma$ polarizations, one can probe the scalar-dominance model via the $J=0$ channel,^{38,45} to compensate the shortcoming in the e^+e^- annihilation.

The SEWS effects in $\gamma\gamma$ colliders mainly go through loop contributions. Signal process $\gamma\gamma \rightarrow W_L^+W_L^-$ has been calculated^{46,47} and the tree level background $\gamma\gamma \rightarrow W_T^+W_T^-$ is found to be larger by about three orders of magnitude. So there is little hope to separate the $W_L^+W_L^-$ mode from the total since there is no effective way of measuring the W^\pm polarization. One may consider to study the $\gamma\gamma \rightarrow Z_LZ_L$ final state since there is no tree-level background. Jikia⁴⁸ first carried out a nice calculation and found that Z_TZ_T final state is still larger than that of Z_LZ_L from a heavy Higgs boson by more than an order of magnitude, as shown in Fig. 8, due to the huge contribution from W^\pm -loop. One could improve the situation by looking at the angular distribution of the fermions from the Z decays, since it goes like $\sin^2\theta_f$ for Z_L and $1+\cos^2\theta_f$ for Z_T at the Z -rest frame with respect to the Z moving

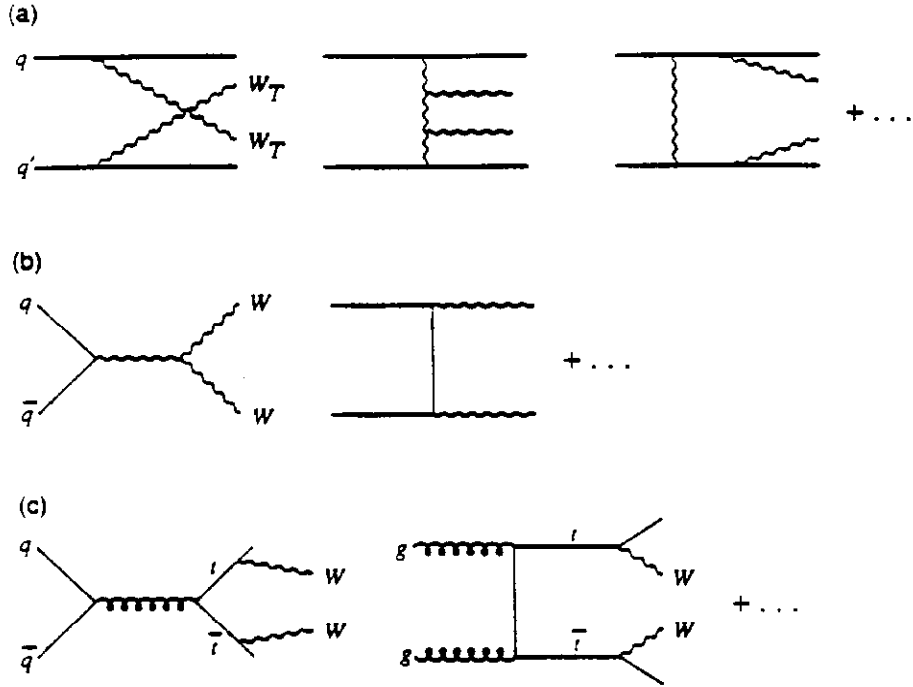


Figure 9: Representative diagrams for backgrounds to the $W_L W_L$ signal: (a) electroweak processes; (b) lowest-order QCD processes, with possible additional QCD-jet radiation; and (c) top-quark backgrounds.

direction. But it is very difficult to achieve an order of magnitude suppression for the $Z_T Z_T$ background. This conclusion has been confirmed more recently.⁴⁹

4. SEWS At Hadronic Supercolliders

The next generation of hadronic supercolliders, such as the SSC (40 TeV) and the LHC (16 TeV), could provide effective c.m. energies as high as a few TeV. This is ideal in searching for the SEWS. Another advantage for hadronic supercolliders over e^+e^- colliders is that, due to the great variety of the partons (quarks and gluons) inside the proton, there are many channels open simultaneously, with different spin, weak-isospin and charge states. However, the major problem with high-energy high-luminosity hadronic colliders is the messy backgrounds. As a comparison, we discuss the prospects of searching for the SEWS at hadronic supercolliders in this section. More details can be found in Ref. 9 as well as the talk presented by Cheung.⁵⁰

Due to the large QCD backgrounds, we are forced to concentrate on the purely leptonic decay modes of the final state W 's, namely the "gold-plated" events, with $W^\pm \rightarrow \ell^\pm \nu_\ell$ and $Z \rightarrow \ell^+ \ell^-$ ($\ell = e, \mu$). The experimental signature is then given by two or more isolated, charged leptons in the central rapidity ($y(\ell)$) region, with large transverse momenta (p_T). Although clean, these gold-plated channels carry

Table 2: Leptonic branching fractions (BR), kinematical cuts, and jet-tag, -veto efficiencies of the signal, for ZZ , W^+W^- , W^+W^+ , and W^+Z channels in the studies of SEWS at the SSC (LHC).

$ZZ (BR = 0.45\%)$	$W^+W^- (BR = 4.7\%)$
$ y_\ell < 2.5$ $p_T > 40 \text{ GeV}$ $p_{Tz} > \frac{1}{4}\sqrt{M_{ZZ}^2 - 4M_Z^2}$ $M_{ZZ} > 500 \text{ GeV}$ tag: $E_j(\text{tag}) > 1(0.8) \text{ TeV}$ $3 < \eta_j(\text{tag}) < 5$ tag eff.: 59(49)%	$ y_\ell < 2$ $p_{T\ell} > 100 \text{ GeV}$ $\Delta p_{T\ell\ell} > 450 \text{ GeV}$ $\cos\phi_{\ell\ell} < -0.8$ $M_{\ell\ell} > 250 \text{ GeV}$ tag: $E_j(\text{tag}) > 1.5(1.0) \text{ TeV}$ $3 < \eta_j(\text{tag}) < 5$ veto: $p_{Tj}(\text{veto}) > 30 \text{ GeV}$ $ \eta_j(\text{veto}) < 3$ veto eff.: 57(40)% veto+tag eff.: 38(24)%
$W^+W^+ (BR = 4.7\%)$	$W^+Z (BR = 1.5\%)$
$ y_\ell < 2$ $p_{T\ell} > 100 \text{ GeV}$ $\Delta p_{T\ell\ell} > 200 \text{ GeV}$ $\cos\phi_{\ell\ell} < -0.8$ $M_{\ell\ell} > 250 \text{ GeV}$ veto: $p_{Tj}(\text{veto}) > 60 \text{ GeV}$ $ \eta_j(\text{veto}) < 3$ veto eff.: 69(58)%	$ y_\ell < 2.5$ $p_{T\ell} > 40 \text{ GeV}$ $p_T > 75 \text{ GeV}$ $p_{Tz} > \frac{1}{4}M_T$ $M_T > 500 \text{ GeV}$ tag: $E_j(\text{tag}) > 2(1.5) \text{ TeV}$ $3 < \eta_j(\text{tag}) < 5$ veto: $p_{Tj}(\text{veto}) > 60 \text{ GeV}$ $ \eta_j(\text{veto}) < 3$ veto eff.: 75(48)% veto+tag eff.: 40(20)%

the price of relatively small branching fractions for the purely leptonic W decays.

The diagram for longitudinal vector boson scattering is given symbolically in Fig. 2. In the case of pp collisions, the initial W_L 's are radiated from light quarks inside a proton. The major backgrounds are symbolically depicted in Fig. 9.

It is important to note that two spectator quarks always emerge in association with the $W_L W_L$ scattering signal, but that spectators emerge in only a subset of the irreducible backgrounds. The spectator quarks usually appear in forward/backward regions, and have an energy of order 1 TeV and a p_T of order $M_W/2$. It is therefore possible to improve the signal/background ratio by tagging those quark jets (in particular, continuum pair production processes do not have a spectator quark jet at lowest order in perturbation theory).⁵¹ While studies have shown that tagging two high p_T spectator jets substantially enhances the signal/background ratio, such double tagging proves to be too costly to the signal.⁵²⁻⁵⁵ It has been recently suggested that tagging just one of these quarks as a single energetic jet can be just as efficient in suppressing the backgrounds that do not intrinsically require spectator jets, and far more efficient in retaining the signal for a heavy Higgs boson.⁵⁵⁻⁵⁷ Thus, to isolate the heavy Higgs and other types of strong $W_L W_L$ signals, we will apply such a forward jet-tag for most final state channels.⁵⁵⁻⁵⁹

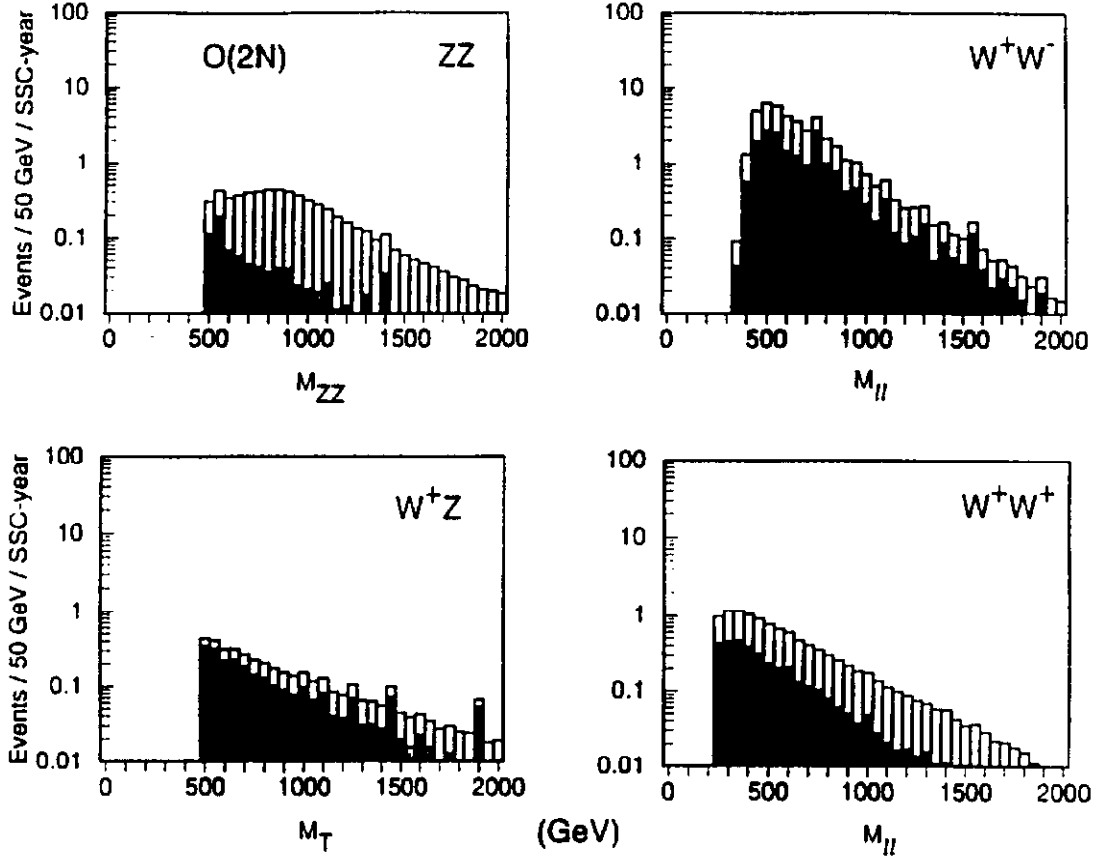


Figure 10: Invariant mass distributions for the $O(2N)$ model with $\Lambda = 3$ TeV for the “gold-plated” leptonic final states that arise from the processes $pp \rightarrow ZZ X$, $pp \rightarrow W^+W^- X$, $pp \rightarrow W^+ Z X$ and $pp \rightarrow W^+W^+ X$, at 40 TeV and an annual SSC luminosity of 10 fb^{-1} . The longitudinally-polarized signal is plotted above the summed background. The mass variable of x -axis is in units of GeV, and the bin size is 50 GeV.

Furthermore, the initial W_L 's participating in the $W_L W_L$ scattering have a $1/(p_T^2 + M_W^2)^2$ distribution with respect to the quarks from which they are emitted. This is to be contrasted, for instance, with $W_T W_T$ scattering where the initiating W_T 's have a $p_T^2/(p_T^2 + M_W^2)^2$ distribution with respect to the emitting quarks. The softer p_T distribution in the $W_L W_L$ case has two primary consequences. First, the spectator quarks left behind tend to emerge with smaller p_T and correspondingly larger rapidity than those associated with the background processes containing spectator jets and $W_L W_T$ or $W_T W_T$ pairs. Therefore we will normally veto hard central jets to enhance the signal/background ratio.^{54,58,59} Such a veto retains most of the signal events. As a further bonus, a central jet-veto is especially effective in suppressing the reducible background from heavy quark production and decay. The jets associated with this latter type of background populate a more central region than do those from spectator quarks. Secondly, the final $W_L W_L$ pair is likely to have much more limited net transverse motion than $W_L W_T$ and $W_T W_T$ pairs produced

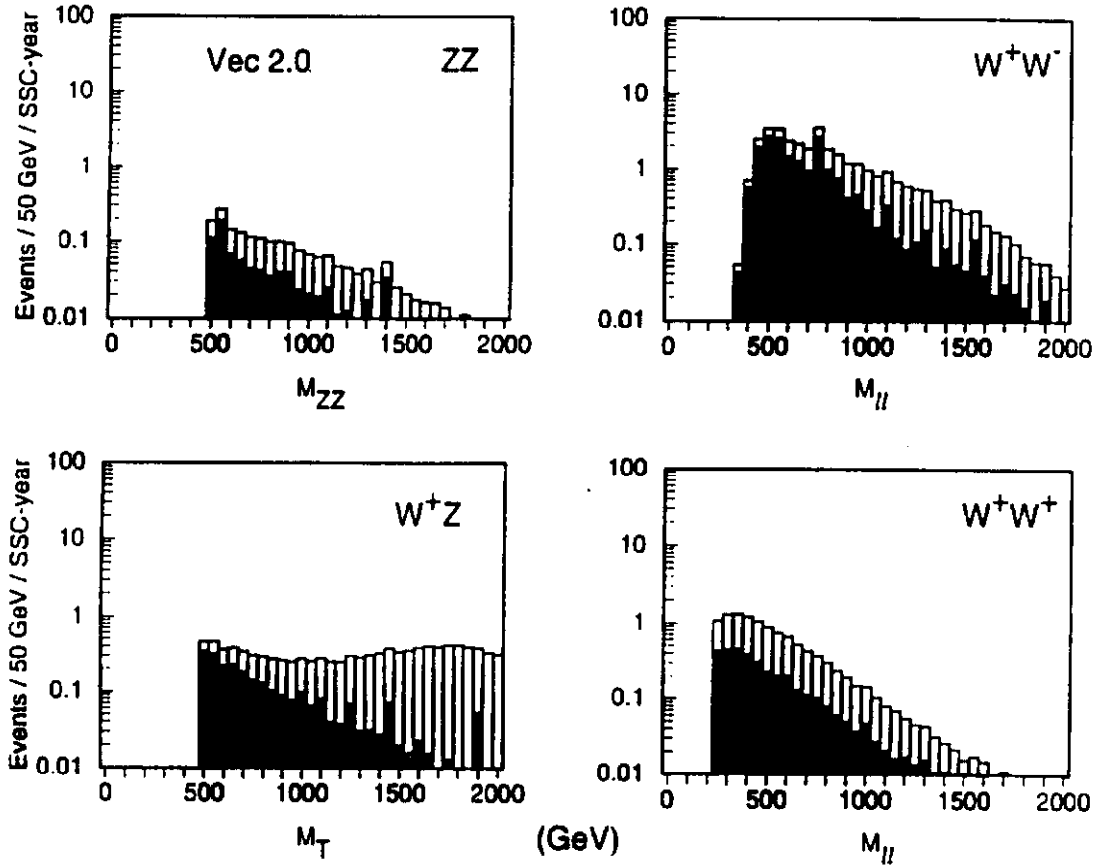


Figure 11: The same as Fig. 10, but for the chirally-coupled vector with $M_V = 2$ TeV, $\Gamma_V = 700$ GeV.

through the various irreducible backgrounds. We then expect the charged leptons from the decays of the two final W_L 's to be very back-to-back in the transverse plane.⁵⁸⁻⁶⁰ This is due not only to the limited p_T of the $W_L W_L$ system but also to the fact that the bulk of the leptons emitted from each final W_L will have a significant (and relatively similar) fraction of the W_L 's total momentum. The latter fact also implies that the leptons will generally be very energetic. A cut requiring that the leptons appearing in the final state be very energetic and very back-to-back will substantially reduce all backgrounds, while being highly efficient in retaining the $W_L W_L$ signal events.

In Table 2, we summarize the leptonic branching fractions, selective kinematical cuts, and jet-tag, -veto efficiencies of the signal, for the ZZ , W^+W^- , W^+W^+ , and W^+Z channels in the studies of SEWS at the SSC (LHC). The signal efficiencies are determined from the full SM calculation with $m_H = 1$ TeV, and are used for other models, assuming that the jet kinematics is essentially independent of specific SEWS models.

It is informative to look at the invariant mass distributions of the $W_L W_L$

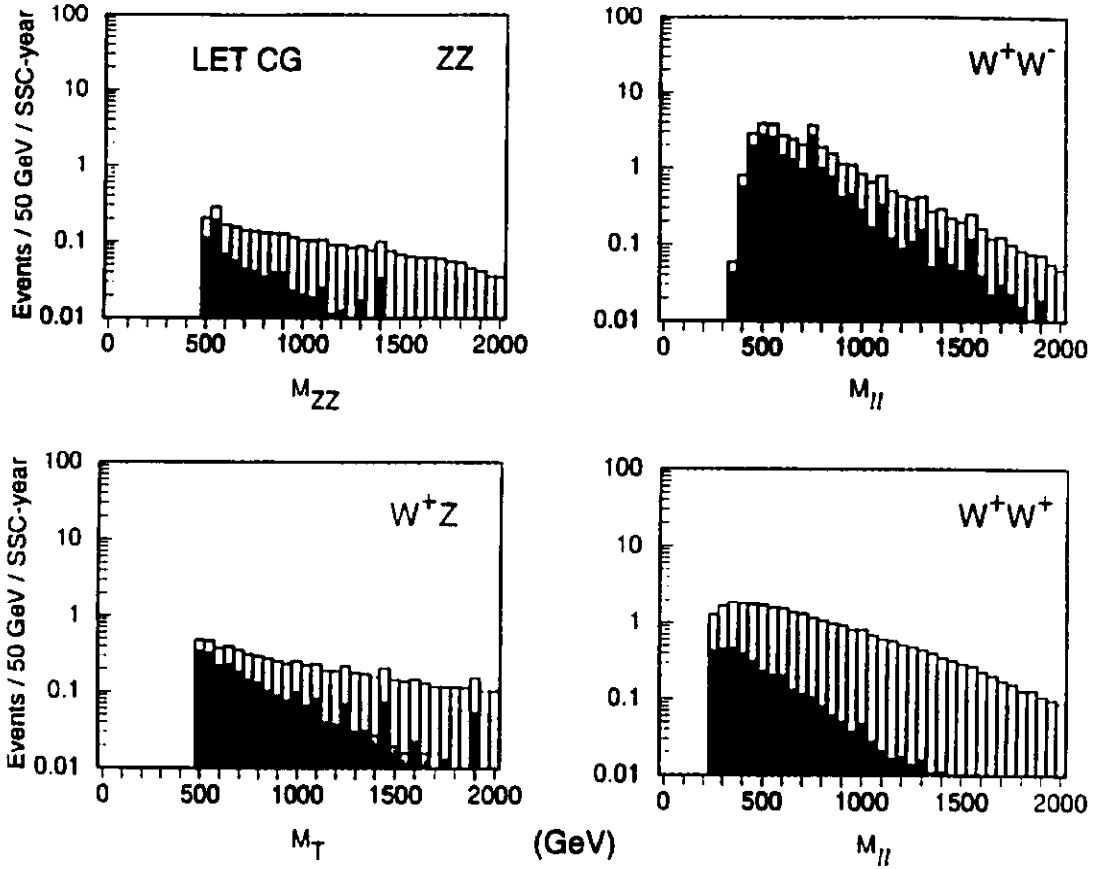


Figure 12: The same as Fig. 10, but for the Nonresonant model unitarized following Chanowitz and Gaillard.

pairs in different channels for different models. In Figures 10-12, we present the invariant mass distributions and WZ cluster transverse mass⁰¹ (M_T) distribution for the $O(2N)$, the chirally-coupled vector and a nonresonance model respectively. One can clearly see the enhancements in W^+W^- and ZZ channels from the scalar-dominance model, in WZ channel from the vector-dominance model (Vector 2.0), and in W^+W^+ channel from a nonresonant LET model.

The results for one-year run at the SSC (LHC), with the three types of SEWS models, are shown in Table 3. We see once again that different channels are sensitive to different types of underlying physics. The W^+W^- and ZZ channels have the largest signal/background ratio for the scalar-dominance models, with W^+W^- having much larger rate. Vector-dominance models are more likely to be discovered in the WZ channel, and W^+W^+ are more sensitive to nonresonant models. To further quantify the observability of the signal over backgrounds, Table 4 shows the number of years needed to observe a particular model for each channel at a 95% Confidence Level, at the SSC (LHC) with an annual luminosity 10 (100) fb^{-1} , calculated by assuming Poisson statistics.⁹ Based on the above discussion, we conclude that

Table 3: Number of events for the “gold-plated” leptonic final states at the SSC (LHC) for an integrated luminosity of 10 (100) fb^{-1} .

	$O(2N)$	Scalar 1.0	Vector 2.0	LET CG	Bckgrnds
ZZ	5.2 (6.4)	6.2 (7.5)	1.1 (1.4)	2.6 (2.5)	1.0 (1.0)
W^+W^-	24 (19)	30 (26)	15 (8.0)	16 (9.2)	21 (18)
W^+Z	1.5 (1.1)	1.8 (1.4)	9.5 (4.8)	5.8 (3.2)	2.5 (2.4)
W^+W^+	7.1 (10)	8.2 (12)	7.8 (12)	25 (27)	3.5 (6.2)

Table 4: Estimated number of SSC (LHC) years needed (if < 10) to observe the SEWS effects at a 95% Confidence Level.

	$O(2N)$	Scalar 1.0	Vector 2.0	LET CG
ZZ	3.0 (2.5)	2.2 (1.8)	- (-)	4.0 (4.8)
W^+W^-	0.75 (1.0)	0.5 (0.75)	1.2 (3.8)	1.2 (3.0)
W^+Z	- (-)	- (-)	0.75 (1.8)	1.8 (4.0)
W^+W^+	2.2 (2.2)	2.2 (1.8)	2.5 (2.0)	0.25 (0.5)

within 1–3 years of running at the SSC (LHC), it is possible to observe the SEWS effects via the $W_L W_L$ scattering in the gold-plated decay modes. All WW' channels must be studied coherently in order to extract the underlying dynamics.

5. Summary

If there are no light Higgs bosons found below $\mathcal{O}(800 \text{ GeV})$ or so, the interactions among longitudinally-polarized vector bosons will become strong at the TeV region, and the new physics that is responsible for the electroweak symmetry breaking must emerge at this energy scale. We have discussed the phenomenological prospects of the SEWS at future linear colliders and hadronic supercolliders.

At a 1.5 TeV e^+e^- collider with an annual integrated luminosity of 200 fb^{-1} , the most straightforward search is for a $(I, J = 1, 1)$ resonance V produced from e^+e^- annihilation via W - V mixing or final state interactions. With a few-year run, we should be able to scan over a substantial part of the parameter space, including the LET case of $M_V \rightarrow \infty$. Unfortunately, a TeV $\gamma\gamma$ collider may not be a good place to probe the $(I, J = 0, 0)$ channel via $W_L^+ W_L^-$ or $Z_L Z_L$ final states, due to the huge $W_T^+ W_T^-$ and $Z_T Z_T$ backgrounds.

$W_L W_L$ fusion processes provide direct access to a variety of channels. At a 1.5 – 2 TeV e^+e^- collider with 200 – 300 fb^{-1} integrated luminosity, it is very promising to observe the SEWS effects via the fusion processes. Due to the inefficient use of the total energy, the signal rate is relatively small and the backgrounds are comparable. More careful studies on the backgrounds are needed before drawing conclusions. We emphasize the importance of effectively distinguishing the hadronic W'^{\pm} and Z decays, in order to examine the underlying dynamics by comparing the $W_L^+ W_L^-$ and

$Z_L Z_L$ processes, as well as to separate certain backgrounds.

Due to the relatively clean environment at e^+e^- colliders, the possibly large inelastic channels of $W_L W_L$ fusion in the "hidden symmetry-breaking sector" could also be studied via the hadronic final state. This would make the e^+e^- colliders complementary to hadronic supercolliders in exploring the SEWS.

At hadronic supercolliders such as the SSC (LHC), the effective c.m. energies are higher, but the environment of the backgrounds is messier. After sophisticated kinematical cuts and with a few tens (hundreds) fb^{-1} integrated luminosity, it is possible to observe the SEWS effects at the SSC (LHC). Due to rather small signal rates, higher luminosity option would be desirable if the faked backgrounds can be kept under control.

Searching for the SEWS seems to be a hard experiment. However, in designing the next generation of colliders and detectors before a light Higgs boson is found, one has to bear this logical possibility of the SEWS in mind.

Acknowledgements

I would like to thank J. Bagger, V. Barger, K. Cheung, J. Gunion, G. Ladinisky, J. Ohnemus, R. Phillips, R. Rosenfeld, C.-P. Yuan, and D. Zeppenfeld for collaborations on the related subjects in the past few years. I am also grateful to M. Chanowitz and K. Hikasa for comments in preparing this talk. Helpful discussions with T. Barklow, D. Burke, E. Boos, D. Dominici, K. Hagiwara, G. Jikia, K. Kanzaki, Y. Kurihara, M. Peskin, C. Quigg, G. Valencia, S. Willenbrock, E. Yehudai are also appreciated. Finally, I would like to thank the conference organizers for a stimulating and enjoyable meeting.

References

1. P. Langacker, Univ. of Pennsylvania Preprint, UPR-0555-T (1993).
2. M. Veltman, *Acta Phys. Polon.* **B8** (1977) 475; B. W. Lee, C. Quigg, and H. Thacker, *Phys. Rev. Lett.* **38** (1977) 883; *Phys. Rev.* **D16** (1977) 1519.
3. M. S. Chanowitz and M. K. Gaillard, *Nucl. Phys.* **B261** (1985) 379.
4. J. M. Cornwall, D. N. Levin, and G. Tiktopoulos, *Phys. Rev.* **D10** (1974) 1145; C. Vayonakis, *Lett. Nuovo Cimento* **17** (1976) 383; G. J. Gounaris, R. Kogerler, and H. Neufeld, *Phys. Rev.* **D34** (1986) 3257; Y.-P. Yao and C.-P. Yuan, *Phys. Rev.* **D38** (1988) 2237; J. Bagger and C. R. Schmidt, *Phys. Rev.* **D41** (1990) 264; H. Veltman, *Phys. Rev.* **D41** (1990) 2294; G. Valencia and S. Willenbrock, *Phys. Rev.* **D42** (1990) 853; H.-J. He, Y.-P. Kuang, and Xiaoyuan Li, *Phys. Rev. Lett.* **69** (1992) 2619.
5. P. Janot, plenary talk in these proceedings.
6. D. A. Dicus and V. S. Mathur, *Phys. Rev.* **D7** (1973) 3111;
7. W. Marciano, G. Valencia, S. Willenbrock, *Phys. Rev.* **D40** (1989) 1725; L.

- Durand, J. Johnson, J. Lopez, *Phys. Rev. Lett.* **64** (1990) 1215; G. Passarino, *Nucl. Phys.* **B343** (1990) 31; L. Durand, J. Johnson, P. N. Maher, *Phys. Rev.* **D44** (1991) 127.
8. for recent reviews on this subject, see *e. g.*, M. Chanowitz, in *Physics at TeV e^+e^- Linear Colliders*, Tsukuba, Japan, 1991, p. 443; LBL-32846 (1992), to be published in *Perspective on Higgs Physics*, ed. G. Kane, World Scientific; K.-I. Hikasa, talk in *Physics and Experiments with Linear Colliders*, Saariselkä, Finland, Sept., 1992, ed. R. Orava *et al.*, World Scientific, p. 451; C.-P. Yuan, MSUTH 92/06, to be published in *Perspective on Higgs Physics*, ed. G. Kane, World Scientific.
 9. J. Bagger, V. Barger, K. Cheung, J. Gunion, T. Han, G. A. Ladinsky, R. Rosenfeld, and C.-P. Yuan, Fermilab Preprint, FERMILAB-PUB-93/040-T (1993).
 10. M. Peskin and T. Takeuchi, *Phys. Rev. Lett.* **65** (1990) 964; *Phys. Rev.* **D46** (1992) 381.
 11. W. Marciano and J. L. Rosner, *Phys. Rev. Lett.* **65** (1990) 2963; D. C. Kennedy and P. Langacker, *Phys. Rev. Lett.* **65** (1990) 2967; G. Altarelli and R. Barbieri, *Phys. Lett.* **B253** (1991) 161; R. D. Peccei and S. Peris, *Phys. Rev.* **D44** (1991) 809.
 12. B. Holdom and J. Terning, *Phys. Lett.* **B247** (1990) 88; M. Golden and L. Randall, *Nucl. Phys.* **B361** (1991) 3; R. Johnson, B.-L. Young, and D. W. McKay, *Phys. Rev.* **D43** (1991) R17; T. Appelquist and G. Triantaphyllou, *Phys. Lett.* **B278** (1992) 345; R. Sundrum and S. D. H. Hsu, *Nucl. Phys.* **B391** (1993) 127.
 13. for a recent review on this subject, see *e. g.*, D. C. Kennedy, Fermilab Preprint, FERMILAB-CONF-93/23-T (1993).
 14. for some recent theoretical discussions on this subject, see *e. g.*, A. De Rújula, M. B. Gavela, P. Hernandez, and E. Massó, *Nucl. Phys.* **B384** (1992) 3; C. P. Burgess and D. London, McGill Univ. Preprint, McGill-92/05 (revised in June, 1993); K. Hagiwara, S. Ishihara, R. Szalapski, and D. Zeppenfeld, UW-Madison Preprint, MAD/PH/737 (1993); and references therein.
 15. J. Bagger, S. Dawson, and G. Valencia, *Nucl. Phys.* **B399** (1993) 364.
 16. M. Einhorn, plenary talk in these proceedings.
 17. J. Gunion, plenary talk in these proceedings; G. Kane, plenary talk in these proceedings.
 18. R. Dashen and H. Neuberger, *Phys. Rev. Lett.* **50** (1983) 1897; J. Kuti, L. Lin, and Y. Shen, *Phys. Rev. Lett.* **61** (1988) 678; M. Luscher and P. Weisz, *Phys. Lett.* **B212** (1988) 472; *Nucl. Phys.* **B318** (1989) 705; U. M. Heller *et al.*, FSU-SCRI-93-29 (1993).
 19. M. Veltman, *Nucl. Phys.* **B123** (1977) 89.
 20. P. Sikivie *et al.*, *Nucl. Phys.* **B173** (1980) 189.

21. S. Weinberg, *Phys. Rev. Lett.* **17** (1966) 616; M. S. Chanowitz, M. Golden, and H. Georgi, *Phys. Rev. Lett.* **57** (1986) 2344; *Phys. Rev.* **D35** (1987) 1149.
22. M. Einhorn, *Nucl. Phys.* **B246** (1984) 75; R. Casalbuoni, D. Dominici, and R. Gatto, *Phys. Lett.* **B147** (1984) 419.
23. S. Weinberg, *Phys. Rev.* **166** (1968) 1568; S. Coleman, J. Wess and B. Zumino, *Phys. Rev.* **177** (1969) 2239; C. Callan, S. Coleman, J. Wess and B. Zumino, *Phys. Rev.* **177**, (1969) 2247; S. Weinberg, *Physica* **96A** (1979) 327.
24. R. Casalbuoni, *et al.*, *Phys. Lett.* **B155** (1985) 95; *Nucl. Phys.* **B282** (1987) 235; see also M. Bando, T. Kugo, and K. Yamawaki, *Phys. Rep.* **164** (1988) 217, and references therein.
25. R. Casalbuoni, *et al.*, *Phys. Lett.* **B269** (1991) 361.
26. D. Dominici, parallel talk in these proceedings.
27. A. Dobado and M. Herrero, *Phys. Lett.* **B228** (1989) 495; A. Dobado, M. Herrero, and J. Terron, *Z. Phys.* **C50** (1991) 205; S. Dawson and G. Valencia, *Nucl. Phys.* **B348**, (1991) 23; *Nucl. Phys.* **B352**, (1991) 27.
28. K.-I. Hikasa and K. Igi, Tohoku Univ. Preprint, TU-428 (1993).
29. S. Dawson and J. Rosner, *Phys. Lett.* **B148** (1984) 497; M. J. Duncan, G. L. Kane, and W. W. Repko, *Nucl. Phys.* **B272**, (1986) 517; **B291**, (1987) 221; G. Altarelli, B. Mele, and F. Pitolli, *Nucl. Phys.* **B287** (1987) 205; M. C. Bento and C. H. Llewellyn Smith, *Nucl. Phys.* **B289**, (1987) 36.
30. J. Gunion and A. Tofighi-Niaki, *Phys. Rev.* **D36** (1987) 2671; *Phys. Rev.* **D38** (1988) 1433.
31. Y. Kurihara and R. Najima, *Phys. Lett.* **B301** (1993) 292.
32. K. Hagiwara, J. Kanzaki, and H. Murayama, Univ. of Durham Preprint, DTP/91/18 (1991). Note that only non-annihilation diagrams were included in this calculation. In the kinematical region of interest, there is essentially no difference between this calculation and that of Ref. 31.
33. A. Dobado and M. J. Herrero, *Phys. Lett.* **B233** (1989) 505, where a rather pessimistic conclusion was drawn.
34. Y. Kurihara, parallel talk in these proceedings.
35. M. S. Chanowitz and M. K. Gaillard, *Phys. Lett.* **B142** (1984) 85; G. L. Kane, W. W. Repko and W. R. Rolnick, *Phys. Lett.* **B148** (1984) 367; S. Dawson, *Nucl. Phys.* **B249** (1985) 42.
36. C. Heusch, parallel talk in these proceedings, and references therein.
37. V. Barger, J. Beacom, K. Cheung, and T. Han, in preparation.
38. M. E. Peskin, talk in *Physics and Experiments with Linear Colliders*, Saariselkä, Finland, Sept., 1992, ed. R. Orava *et al.*, World Scientific, p. 1.
39. D. L. Burke, talk in *Physics and Experiments with Linear Colliders*,

- Saariselkä, Finland, Sept., 1992, ed. R. Orava *et al.*, World Scientific, p. 51.
40. R. S. Chivukula and M. Golden, *Phys. Lett.* **B267** (1991) 233; S. G. Naculich and C.-P. Yuan, *Phys. Lett.* **B293** (1992) 405.
 41. M. E. Peskin, in *Physics in Collisions IV*, ed. A. Seiden (Éditions Frontières, Gif, 1984); F. Iddir, A. Le Yaouanc, L. Oliver, O. Pene, and J. C. Raynal, *Phys. Rev.* **D41** (1990) 22.
 42. T. Barklow, parallel talk in these proceedings, SLAC-PUB-6280 (1993); and talk in *Physics and Experiments with Linear Colliders*, Saariselkä, Finland, Sept., 1992, ed. R. Orava *et al.*, World Scientific, p. 429.
 43. J. L. Basdevant, E. L. Berger, D. Dicus, C. Kao, and S. Willenbrock, Argonne Lab Preprint, ANL-HEP-PR-92-93 (1992), to appear in *Phys. Lett.* **B**.
 44. I. F. Ginzburg, G. L. Kotkin, V. G. Serbo and V. I. Telnov, *Nucl. Instrum. and Methods* **205** (1983) 47; *ibid* **219** (1984) 5; V. I. Telnov, *Nucl. Instrum. and Methods* **A294** (1990) 72.
 45. C. Im, *Phys. Lett.* **B281** (1992) 357.
 46. E. E. Boos and G. V. Jikia, *Phys. Lett.* **B275** (1992) 164.
 47. A. Abbasabadi *et al.*, Michigan State Univ. Preprint, MSUTH 92/03 (1992).
 48. G. V. Jikia, *Phys. Lett.* **B298** (1992) 224; and parallel talk in these proceedings.
 49. M. Berger, UW-Madison Preprint, MAD/PH-771 (1993).
 50. K. Cheung, parallel talk in these proceedings.
 51. R. N. Cahn *et al.*, *Phys. Rev.* **D35** (1987) 1626; R. Kleiss and W. J. Stirling, *Phys. Lett.* **B200** (1988) 193; V. Barger, T. Han, and R. J. N. Phillips, *Phys. Rev.* **D37** (1988) 2005.
 52. D. Froideveaux, *Proceedings of the LHC Workshop*, (1990), CERN 90-10, Vol II, p. 444; M. H. Seymour, *ibid*, p. 557.
 53. U. Baur and E. W. N. Glover, *Nucl. Phys.* **B347** (1990) 12; U. Baur and E. W. N. Glover, *Phys. Lett.* **B252** (1990) 683.
 54. V. Barger, K. Cheung, T. Han, and R. J. N. Phillips, *Phys. Rev.* **D42** (1990) 3052.
 55. V. Barger, K. Cheung, T. Han, J. Ohnemus, and D. Zeppenfeld, *Phys. Rev.* **D44** (1991) 1426.
 56. V. Barger, K. Cheung, T. Han, and D. Zeppenfeld, *Phys. Rev.* **D44** (1991) 2701; Erratum to appear in *Phys. Rev. D*; UW-Madison Preprint, MAD/PH/757.
 57. V. Barger, K. Cheung, T. Han, A. Stange, and D. Zeppenfeld, *Phys. Rev.* **D46** (1992) 2028.
 58. D. Dicus, J. F. Gunion, and R. Vega, *Phys. Lett.* **B258** (1991) 475.
 59. D. Dicus, J. F. Gunion, L. H. Orr, and R. Vega, *Nucl. Phys.* **B377** (1991)

31.

60. M. S. Berger and M. S. Chanowitz, *Phys. Lett.* **B263** (1991) 509.

61. V. Barger, A. D. Martin, and R. J. N. Phillips, *Phys. Lett.* **B125** (1983) 339;
V. Barger, T. Han, and J. Ohnemus, *Phys. Rev.* **D37** (1988) 1174.